Int. J. Heat Mass Transfer. Vol. 9, pp. 1021–1046. Pergamon Press 1966. Printed in Great Britain

THE MECHANISM OF NUCLEATE BOILING IN PURE LIQUIDS AND IN BINARY MIXTURES—PART II

S. J. D. VAN STRALEN†
Heat Transfer Section, Technological University, Eindhoven, The Netherlands

(*Received* 14 *January* 1966)

Abstract—Nucleate boiling is described as a relaxation phenomenon concerning the superheating of the equivalent conduction layer at the heating surface due to the rapid growth of succeeding vapour bubbles on active nuclei.

Expressions for the adherence and delay times, the bubble frequency, the departure radius, the vaporized mass and diffusion fractions at the heating surface, and the nucleate boiling peak flux, could thus be derived. The theoretical predictions are in good agreement with experimental data deduced from high speed motion pictures and from boiling curves on water–methylethylketone and water–1-butanol mixtures.

In addition, a criterion for the onset of film boiling has been formulated in terms of the region of influence of a bubble. The effects of wetting and nucleation are established and incorporated in the theoretical treatment.

The advantage of the present equations over correlations resulting from dimensional analysis is that they reveal a number of highly interesting phenomena, which were obscured previously.

For instance, the theory predicts a coincidence of a maximal slowing down of bubble growth rate and departure size (resulting in a minimal heat transmission to individual bubbles: "boiling paradox") and the occurrence of a maximum nucleate boiling peak flux at the same low concentration of the more volatile component in a binary system, which can be derived from equilibrium data. This is also in accordance with experimental results.

In principle, the theoretical predictions include the favourable effect on peak flux by all other methods resulting in a diminished vapour production at the heating surface—which corresponds generally with an increased frequency of smaller bubbles—e.g. surface boiling, vortex flow, the use of high pressures and the application of an electrostatic field.

1. SUPERHEATING OF THE MICROLAYER DURING THE DELAY TIME

Newton's law can also be used for the derivation of the superheating ϑ of the microlayer during the delay time:

$$C_i \frac{\mathrm{d}\vartheta}{\mathrm{d}t} = A_i h_{w,i}(\vartheta_0 - \vartheta), \tag{1}$$

where A_i denotes the contact area of the microlayer with the heating surface, and is called the "region of influence" of a vapour bubble.

$$C_i = A_i \rho_1 c d_0$$

denotes the heat capacity of the microlayer.

For the present, we solve instead of (1) the related equation:

$$C_i \frac{\mathrm{d}\vartheta^*}{\mathrm{d}t} = A_i h^*_{w,i}(\vartheta_0 - \vartheta^*), \tag{2}$$

where ϑ^* is defined by

$$\vartheta^* = \vartheta - \frac{\vartheta_0}{\mathrm{e}}. \tag{3}$$

† Doctor of Physics, Principal Research Officer.

It follows from equation (2) that:

$$\frac{d\vartheta^*}{dt} = A_i \frac{k}{(\pi at)^{\frac{1}{2}}} \frac{1}{A_i \rho_1 c d_0} (\vartheta_0 - \vartheta^*) = f_i(\vartheta_0 - \vartheta^*)t^{-\frac{1}{2}}, \tag{4}$$

where for abbreviation

$$f_i = \frac{k}{(\pi a)^{\frac{1}{2}}} \frac{1}{\rho_1 c d_0}. \tag{5}$$

For the coefficient of heat transfer

$$h^*_{w,i} = \frac{k}{(\pi at)^{\frac{1}{2}}} \tag{6}$$

the value for heat conduction to a semi-infinite liquid body with a sudden change in surface temperature, is taken here.

The general solution of the inhomogeneous linear differential equation of the first order (4) is:

$$\vartheta = D_2 \exp(-2f_i t^{\frac{1}{2}}) + \vartheta_0(1 + 1/e).$$

The required particular solution has to satisfy the conditions: (i) initially, $\vartheta(0) = \vartheta_0/e$, where $t = 0$ is taken at the instant of departure of the preceding bubble on the same nucleus, and (ii) $\vartheta(t_2) = \vartheta_0$, as the succeeding bubble will be generated on the nucleus at this superheating; this is in agreement with the periodic character of bubble formation. The quantity $\vartheta_0 - \vartheta^*$ in equation (2) varies during heating from ϑ_0 to ϑ_0/e, i.e. necessarily over the same temperature difference as during cooling [1]. The required solution following from the condition (i) is:

$$\vartheta = \vartheta_0/e + \vartheta_0 \{1 - \exp[-(t/t_2)^{\frac{1}{2}}]\} \tag{7}$$

i.e. $D_2 = -\vartheta_0$ and it follows from (ii) that:

$$u_2 = t_2^{\frac{1}{2}} = \frac{1}{2f_i} = \frac{(\pi a)^{\frac{1}{2}}}{2k} \rho_1 c d_0 = \frac{(\pi a)^{\frac{1}{2}}}{2k} \rho_2 l C_1 u_1, \tag{8}$$

or, generally for binary mixtures:

$$u_2 = \frac{(\pi a)^{\frac{1}{2}}}{2k} \rho_2 l \left(\frac{12}{\pi}\right)^{\frac{1}{2}} \frac{a^{\frac{1}{2}}}{\frac{\rho_2 l}{\rho_1 c}\left\{1 + \frac{c}{l}\left(\frac{a}{D}\right)^{\frac{1}{2}} \frac{\Delta T}{G_d}\right\}} = \frac{3^{\frac{1}{2}}}{1 + \frac{c}{l}\left(\frac{a}{D}\right)^{\frac{1}{2}} \frac{\Delta T}{G_d}} u_1. \tag{9}$$

The solution (7) for the microlayer superheating (Fig. 1) is also the required solution of equation (1), which follows by taking:

$$h_{w,i} = \frac{\vartheta_0 - \vartheta^*}{\vartheta_0 - \vartheta} h^*_{w,i} = \frac{\vartheta_0(1 + 1/e) - \vartheta}{\vartheta_0 - \vartheta} \frac{k}{(\pi at)^{\frac{1}{2}}}. \tag{10}$$

This corresponds with a local surface heat flux density

$$q_{w,i} = (\vartheta_0 - \vartheta)h_{w,i} = [k/(\pi at)^{\frac{1}{2}}]\, \vartheta_0 \exp[-(t/t_2)^{\frac{1}{2}}]. \tag{11}$$

The average value of $q_{w,i}$ during the delay time is, cf. equation (17):

$$\bar{q}_{w,i} = \frac{1}{t_2} \frac{k\vartheta_0}{(\pi a)^{\frac{1}{2}}} \int_0^{t_2} t^{-\frac{1}{2}} \exp\left[-\left(\frac{t}{t_2}\right)^{\frac{1}{2}}\right] dt = 2 \frac{k}{(\pi a t_2)^{\frac{1}{2}}} \vartheta_0 \left(1 - \frac{1}{e}\right) = \frac{4}{\pi} \frac{k}{d_0} \vartheta_0 \left(1 - \frac{1}{e}\right),$$

whence, in combination with equations (8) and (19), the maximal excess enthalpy—which is accumulated in the relaxation microlayer at the instant t_2—amounts to:

$$\Delta H_0 = \bar{q}_{w,i} t_2 A_i = \frac{8\pi}{3} \frac{k}{(\pi a)^{\frac{1}{2}}} \vartheta_0 t_2^{\frac{1}{2}} \frac{b}{e} R_1^2 = \frac{4\pi}{3} \rho_2 l R_1^3, \tag{12}$$

i.e. equation (18), cf. Section 1.3.

It may be worth reporting here, that $\bar{q}_{w,i}$ for one individual bubble is obviously connected with the contribution $q_{w,b}$ to the total heat flux density of the entire direct vapour formation at the heating surface (Section 4.1):

$$q_{w,b} = \frac{m}{A_w} \frac{4\pi}{3} \rho_2 l R_1^3 \nu = \frac{m}{A_w} \bar{q}_{w,i} t_2 A_i \nu.$$

One has thus for a pure liquid—equation (13)—at peak flux conditions—equation (64)—the expression:

$$q_{w,b,\max} = \tfrac{3}{4} \bar{q}_{w,i,\max} = \frac{3}{\pi} \frac{k}{d_0} \vartheta_{0,\max} \left(1 - \frac{1}{e}\right) = \tfrac{1}{2} \left(\frac{3}{\pi}\right)^{\frac{1}{2}} \frac{k}{(a t_1)^{\frac{1}{2}}} \vartheta_{0,\max} \left(1 - \frac{1}{e}\right),$$

i.e. equation (66) in combination with equation (67).

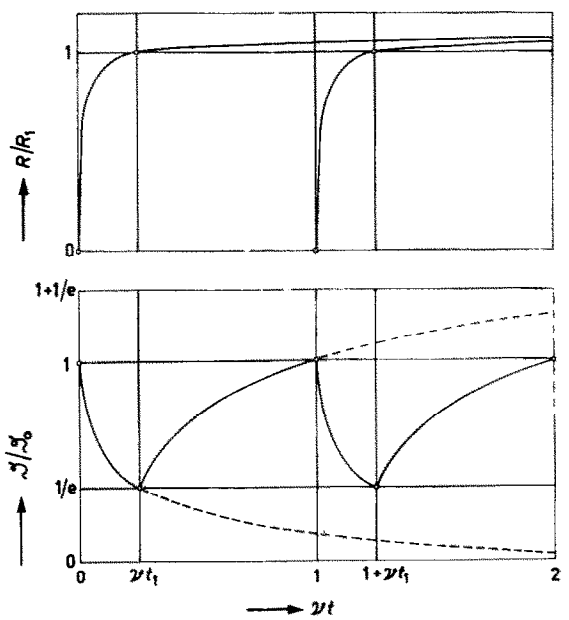

FIG. 1. Dimensionless growth curves of succeeding bubbles on same nucleus, and corresponding superheating of relaxation microlayer.

1.1 *Pure liquids*

For pure liquids (and azeotropic mixtures) $\Delta T/G_d = 0$, whence equation (9) is simplified to:

$$u_2 = (\sqrt{3})u_1$$

or

$$t_2 = 3t_1. \tag{13}$$

The frequency of bubble formation on a nucleus amounts to:

$$\nu = \frac{1}{t_1 + t_2} = \frac{1}{4t_1} = \frac{3}{4t_2}. \tag{14}$$

It is seen now, that the quantity

$$\nu R_1^2 = \frac{1}{4u_1^2}\left(\frac{b}{e} C_1 \vartheta_0 u_1\right)^2 = \left(\frac{b}{2e} C_1 \vartheta_0\right)^2 \tag{15}$$

is independent of the instant of departure t_1, and consequently a constant for all nuclei generating bubbles on a heating surface of uniform superheating. In this case, νR_1^2 is proportional to C_1^2, whence a minimum of this quantity is predicted to occur in binary mixtures with minimum C_1, i.e. in those mixtures with minimum bubble growth rates. Further, νR_1^2 increases with increasing ϑ_0 in the region of nucleate boiling. The validity of the theory can also be checked now by making a comparison of the quantity νR_1^2 with experimental values, cf. Table 1 (Appendix).

Empirical relations similar to equation (15) are known in the literature, e.g. $\nu R_1 =$ constant, for any liquid according to Jakob [2, 3], a statement based on measurements on water and carbontetrachloride only, or $\nu R_1^3 =$ constant, according to investigations by Rallis and Jawurek [4] on water. The bubble frequency on a nucleus increases with decreasing bubble departure size, according to all three equations. It is predicted here, that νR_1^2 is affected by ϑ_0; this has previously not been taken into consideration. Equation (15) supersedes the empirical relations of previous workers.

1.2 *Binary mixtures*

One has, more generally, for bubbles generated in superheated binary mixtures:

$$\nu = \frac{1}{[1 + (\pi a/4k^2)\rho_2^2 l^2 C_1^2]t_1}, \tag{16}$$

whence the expression

$$\nu R_1^2 = \frac{[(b/e)C_1\vartheta_0]^2}{1 + (\pi a/4k^2)\rho_2^2 l^2 C_1^2}$$

is also in this general case independent of t_1 and t_2.
One can make use of the approximation:

$$\nu R_1^2 \approx [(b/e)C_1\vartheta_0]^2$$

for mixtures with a small growth constant, e.g. for 4·1 wt. % methylethylketone in water ($C_1 = 6 \times 10^{-4}$ m/s$^{\frac{1}{2}}$ degC); this equals thus 25 per cent of the value of νR_1^2 in water, c.f. the Appendix.
It follows from equation (8), that

$$d_0 = \frac{1}{\rho_1 c}\frac{2k}{(\pi a)^{\frac{1}{2}}} u_2 = \frac{2}{\pi}(\pi a t_2)^{\frac{1}{2}}, \tag{17}$$

whence $d_0/2$ equals the average thickness of the equivalent conduction layer during the delay time for constant heat flux density at the surface, cf. Carslaw and Jaeger [5].

1.3 *The region of influence of a vapour bubble*

It is impossible to derive the contact area A_i of the microlayer with the heating surface during the delay time (waiting period) directly from Newton's extended cooling law, as the heat capacity C_i of the microlayer is proportional with A_i. Consequently, we make use of the integral over the left-hand side of equation (1), i.e. the excess enthalpy balance assuming time-independence of A_i during local heating:

$$\Delta H_0 = \int_0^{t_2} C_i \frac{\mathrm{d}\vartheta}{\mathrm{d}t}\,\mathrm{d}t = \int_{\vartheta_0/e}^{\vartheta_0} C_i\,\mathrm{d}\vartheta = C_i\vartheta_0\left(1-\frac{1}{e}\right) = A_i\rho_1 c d_0\vartheta_0\left(1-\frac{1}{e}\right) = \frac{4\pi}{3}\rho_2 l R_1^3, \quad (18)$$

or

$$A_i C_1\vartheta_0\left(1-\frac{1}{e}\right)u_1 = \frac{4\pi}{3}R_1^2\left(\frac{b}{e}C_1\vartheta_0 u_1\right),$$

whence

$$A_i = \frac{4\pi}{3(e-1)}bR_1^2. \quad (19)$$

The same result can, of course, be obtained by integrating the right-hand side of equation (1), cf. equation (12):

$$\Delta H_0 = A_i\int_0^{t_2} h_{w,i}(\vartheta_0-\vartheta)\,\mathrm{d}t = A_i\int_0^{t_2} h^*_{w,i}(\vartheta_0-\vartheta^*)\,\mathrm{d}t = A_i\bar{q}_{w,i}t_2 = (4\pi/3)\rho_2 l R_1^3.$$

For bubbles with $b = 0{\cdot}70$, the radius of the region of influence A_i amounts to $R_i = 0{\cdot}74\,R_1$ and its area to $\pi R_i^2 = 1{\cdot}71\,R_1^2$.

1.4 *Comparison of the average volume of the microlayer during heating and cooling*

It is seen from equation (36) of Part I of this paper, that the volume of the microlayer, which is pushed away from the heating surface during initial bubble growth, amounts to:

$$V = 4\pi bR^2 d = 4\pi b^3 C_1^3\vartheta_0^2\frac{\rho_2 l}{\rho_1 c}(u_1u^2-u^3)\exp\left(-2\frac{u}{u_1}\right) = D_3(u_1u^2-u^3)\exp\left(-2\frac{u}{u_1}\right), \quad (20)$$

whence the average cooling liquid volume adjacent to the bubble is:

$$\bar{V} = \frac{D_3}{t_1}\int_0^{t_1}(u_1u^2-u^3)\exp\left(-2\frac{u}{u_1}\right)\mathrm{d}t = \frac{D_3}{t_1}2\int_0^{u_1}(u_1u^3-u^4)\exp\left(-2\frac{u}{u_1}\right)\mathrm{d}u$$

$$= \frac{D_3}{u_1^2}\frac{u_1^5}{16}\int_0^2(2\xi^3-\xi^4)\exp(-\xi)\,\mathrm{d}\xi \quad (21)$$

by introducing the dimensionless integration variable

$$\xi = \frac{2}{u_1} u. \tag{22}$$

One can now make use of the recurrence formula:

$$\int \xi^n \exp(-\xi)\, d\xi = -\exp(-\xi)\{\xi^n + n\xi^{n-1} + n(n-1)\xi^{n-2} + \ldots + n!\},$$

whence

$$\bar{V} = \frac{D_3}{16} u_1^3 \{(\xi^4 + 2\xi^3 + 6\xi^2 + 12\xi + 12)\exp(-\xi)\}\Big|_0^2 = \frac{D_3}{16} u_1^3 \left(\frac{92}{e^2} - 12\right)$$

$$= \frac{1}{16} u_1^3 \left(\frac{92}{e^2} - 12\right) 4\pi b^3 C_1^3 \vartheta_0^2 \frac{\rho_2 l}{\rho_1 c} = \frac{1}{16}(92 - 12e^2) 4\pi b R_1^2 d_0$$

$$= 0{\cdot}208\,(4\pi b R_1^2 d_0). \tag{23}$$

This must be compared with the microlayer volume, which is superheated during the delay time:

$$A_i d_0 = \frac{1}{3(e-1)} 4\pi b R_1^2 d_0 = 0{\cdot}194\,(4\pi b R_1^2 d_0) \tag{24}$$

whence

$$\bar{V} = 1{\cdot}07\, A_i d_0, \tag{25}$$

i.e. there is good agreement of the volume as calculated by both methods.

1.5 *Relation between microlayer and conduction boundary layer at the heating surface*

The excess enthalpy of the microlayer in a pure liquid, which is removed from the heating surface due to the initial rapid bubble growth, must be required from the heat storage in the equivalent conduction boundary layer with a linear temperature profile at the wall. One has thus:

$$\Delta H_0 = \frac{4\pi}{3} \rho_2 l R_1^3 = A_i \rho_1 c d_{0,p} \vartheta_0 \left(1 - \frac{1}{e}\right) \leqslant A_i \rho_1 c d_w \frac{\vartheta_0}{2}, \tag{26}$$

or approximately:

$$d_{0,p} \vartheta_0 \left(1 - \frac{1}{e}\right) \leqslant d_w \frac{\vartheta_0}{2} = \frac{k}{2h_w} \vartheta_0, \tag{27}$$

whence

$$d_{0,p} \leqslant \frac{e}{2(e-1)} d_w = 0{\cdot}79\, d_w. \tag{28}$$

The coefficient of heat transfer h_w from the heating surface to the liquid has to be taken here at the

superheating ϑ_0, but can generally be approximated by the value at the transition point on the boiling curve between convection and nucleate boiling.

However, in a binary mixture, which contains the less volatile component in excess (i.e. restriction has been made to mixtures of which the thermal quantities differ only slightly from the values in the main pure component), one has obviously

$$d_{w,m} = d_{w,p} = d_w,$$

and consequently, cf. equation (36):

$$d_{0,m} \leqslant \frac{e}{2(e-1)} \frac{C_{1,m} u_{1,m}}{C_{1,p} u_{1,p}} d_w = 0{\cdot}79 \frac{C_{1,m}}{C_{1,p}} d_w. \tag{29}$$

In water, for instance, $d_{0,p} = 63\ \mu$ (Table 1 of Part I of this paper) and $d_w = 75\ \mu$ follows from the boiling curve at the transition between convection and nucleate boiling in the special boiling vessel used for high speed motion pictures, cf. Figs. 3 and 4 of [1] [cf. also equation (17) and, e.g. bubble *a* in water—Table 1—with $(\pi a t_2)^{\frac{1}{2}} = 76\ \mu$], whence both sides of equations (26)–(29) are identical. In this case the entire excess enthalpy of the thermal boundary layer, which has been pushed away from the heating surface, is obviously used for direct vaporization at the surface. The whole increase in heat flux in the region of nucleate boiling above (free or forced) convection, which is caused by the action of the bubbles, is only due to the direct vapour formation at the heater.

Apparently, this is in sharp contrast to the behaviour of binary mixtures, where the excess enthalpy of the thermal layer is only partly consumed for direct vaporization. In 4·1 wt. % methylethylketone, the vapour formation at the heating surface amounts to only approximately 25 per cent (because of $C_{1,m} = 0{\cdot}25\, C_{1,p}$ here) of the total bubble-induced increase in heat flux, cf. Table 3. The remaining part of the thermal energy stored in the boundary layer is transmitted to the adjacent colder bulk liquid. Similar situations can be expected to occur in surface boiling of subcooled liquids, where the vapour formation is restricted due to subsequent condensation.

2. THE VAPORIZED FRACTION AT THE HEATING SURFACE

2.1 *The vaporized mass fraction*

The mass fraction G_h for individual vapour bubbles, which is vaporized at the heating surface†, is defined by the ratio of the bubble mass at the instant of departure to the mass of the associated thermal microlayer:

$$G_h = \frac{(4\pi/3)\rho_2 R_1^3}{A_i d_0 \rho_1} = \frac{(4\pi/3)\rho_2 l R_1^3}{A_i d_0 \rho_1 \vartheta_0 (1 - 1/e) c} \frac{c\vartheta_0(1-1/e)}{l} = \frac{c}{l}\vartheta_0\left(1 - \frac{1}{e}\right), \tag{30}$$

i.e. this quantity, which has an exact physical meaning here, is independent of the bubble growth constant C_1 and has consequently the same value for binary mixtures and the pure less volatile component.

However, the vaporized mass fraction G_d of original liquid, which follows from the theory of

† The analogous definition of G_h as applied to the vaporized mass fraction on a nucleus is identical on account of the periodic formation of bubbles of constant size. The influence of one active nucleus on the whole area A_w of the heating surface is given by the ratio $G'_h = (A_i/A_w)(c/l)\,\vartheta_0(1 - 1/e)$. One has at the peak flux for all active nuclei per unit area together: $G''_{h,\max} = m_{\max} G'_{h,\max} = (c/l)\vartheta_{0,\max}(1 - 1/e) = G_{h,\max}$, as $m_{\max}/A_w = 1/A_i$, cf. the present criterion for the onset of film boiling, Section 3.3.

bubble growth in binary mixtures, is given by the expression [6]:

$$G_d = \frac{\rho_2}{\rho_1}\varphi(\varepsilon, \mu\beta) = \frac{\rho_2}{\rho_1}\mu\varphi(\varepsilon, \beta) = \frac{\rho_2}{\rho_1}\left(\frac{\pi}{3}\right)^{\frac{1}{2}}\left(\frac{a}{D}\right)^{\frac{1}{2}}\frac{C_{2,m}}{2a^{\frac{1}{2}}} = \left(\frac{\pi}{12}\right)^{\frac{1}{2}}\frac{\rho_2}{\rho_1}\frac{C_{1,m}}{D^{\frac{1}{2}}}\vartheta_0\left(1 - \frac{1}{e}\right)$$
$$= \left(\frac{\pi}{12}\right)^{\frac{1}{2}}\frac{\rho_2}{\rho_1}\frac{1}{D^{\frac{1}{2}}}\vartheta_0\left(1 - \frac{1}{e}\right)C_{1,p}\frac{C_{1,m}}{C_{1,p}} = \left(\frac{a}{D}\right)^{\frac{1}{2}}\frac{c}{l}\vartheta_0\left(1 - \frac{1}{e}\right)\frac{C_{1,m}}{C_{1,p}}$$
$$= \left(\frac{a}{D}\right)^{\frac{1}{2}}\frac{C_{1,m}}{C_{1,p}}G_h = \left(\frac{a}{D}\right)^{\frac{1}{2}}G_h^* = \mu G_h^*, \tag{31}$$

where the corresponding fraction G_h^* is defined by:

$$G_h^* = \frac{C_{1,m}}{C_{1,p}}G_h \leqslant G_h. \tag{32}$$

Equations (31) and (32) can also be derived from the well-known analogy between heat and diffusion. The equation governing the concentration follows from the heat conduction equation by replacing β by $\mu\beta = (a/D)^{\frac{1}{2}}\beta$, i.e. the vaporized mass fraction G_h^* for heat can be calculated by multiplying G_d with $1/\mu = (D/a)^{\frac{1}{2}}$, whence:

$$G_h^* = \frac{\rho_2}{\rho_1}\varphi(\varepsilon, \beta) = \frac{\rho_2}{\rho_1}\left(\frac{\pi}{3}\right)^{\frac{1}{2}}\frac{C_{2,m}}{2a^{\frac{1}{2}}} = \frac{c}{l}\vartheta_0\left(1 - \frac{1}{e}\right)\frac{C_{1,m}}{C_{1,p}} = \frac{C_{1,m}}{C_{1,p}}G_h. \tag{33}$$

It may be worth reporting, that the same result can be obtained even more easily from the definitions of the thermal fraction G_h according to equation (30) and of the diffusion fraction

$$G_d = (x_0 - x)/(y - x) = (x_0 - x)/(K - 1)x,$$

since the thermal quantities c/l and $\vartheta_0(1 - 1/e)$ are analogous to the diffusion quantities $1/(K - 1)x$ and $x_0 - x$ respectively [6].

One has to consider here, that G_h applies to that part of the removed thermal microlayer adjacent to the boundary of the growing bubble, the excess enthalpy of which equals the total energy required for vaporization into the bubble space up to the instant of departure. The thickness of this layer is in binary mixtures smaller than in pure liquids, cf. Section 1.5 and Table 1 of [1].

Contrarily, G_h^* applies to the whole thickness of the thermal microlayer, which is removed from the heating surface during the initial growth of the bubble adhering to the surface, i.e. both in pure liquids and in binary mixtures to the relaxation microlayer of the pure liquid, the excess enthalpy of which equals that of the equivalent conduction layer; hence $G_h^* = G_h$ for pure liquids and $G_h^* \leqslant G_h$ for mixtures.

One has thus for mixtures with a low concentration of the more volatile component:

$$G_h^* = \frac{(4\pi/3)\rho_2 R_1^3}{A_i d_{0,p}\rho_1} = \frac{(4\pi/3)\rho_2 R_1^3}{A_i d_{0,m}\rho_1}\frac{d_{0,m}}{d_{0,p}} = G_h\frac{(\rho_2 l/\rho_1 c)C_{1,m}u_{1,m}}{(\rho_2 l/\rho_1 c)C_{1,p}u_{1,p}} = \frac{C_{1,m}u_{1,m}}{C_{1,p}u_{1,p}}G_h, \tag{34}$$

or, in combination with equation (29):

$$\frac{C_{1,m}u_{1,m}}{C_{1,p}u_{1,p}} = \frac{G_h^*}{G_h} = \frac{d_{0,m}}{d_{0,p}} = 2\left(1 - \frac{1}{e}\right)\frac{d_{0,m}}{d_w}. \tag{35}$$

It is seen by comparing equations (33) and (34), that

$$u_{1,m} = u_{1,p} \tag{36}$$

whence

$$t_{1,m} = t_{1,p}, \tag{37}$$

i.e. the departure time is independent of the composition of the mixture. This is in agreement with experimental data, cf. Table 1 of Part I of this paper. Equation (37) is valid for bubbles generated on "ordinary" nuclei.

For bubbles generated on "complex" nuclei, one has $C_{1,c} = (\frac{1}{2})C_{1,m}$ (cf. Section 3.17 of Part I of this paper), whence

$$R_{1,c} = \tfrac{1}{2}\frac{b}{\mathrm{e}} C_{1,m}\vartheta_0 u_{1,c} = \frac{b}{\mathrm{e}} C_{1,c}\vartheta_0 u_{1,c} \tag{38}$$

and

$$G_{h,c} = G_h = \frac{c}{l}\vartheta_0\left(1 - \frac{1}{\mathrm{e}}\right). \tag{30}$$

The ratio

$$\frac{G^*_{h,c}}{G_{h,c}} = \frac{(\rho_2 l/\rho_1 c)C_{1,m}u_{1,c}}{(\rho_2 1/\rho_1 c)C_{1,p}u_{1,p}} = 2\frac{C_{1,c}u_{1,c}}{C_{1,p}u_{1,p}}. \tag{39}$$

On the other hand:

$$\frac{G^*_{h,c}}{G_{h,c}} = \frac{C_{1,c}}{C_{1,p}} \tag{40}$$

whence

$$2u_{1,c} = u_{1,p} \tag{41}$$

or

$$t_{1,c} = \tfrac{1}{4}t_{1,p} = \tfrac{1}{4}t_{1,m}, \tag{42}$$

which result is quite satisfactory since it agrees reasonably with the experimental data, cf. Table 1 of Part I of this paper.

2.2 *The vaporized diffusion fraction*

It is seen from equation (30), that G_h is independent of u_1 and C_1, and practically independent of the composition of the binary mixture, which contains the less volatile component in excess, at constant ϑ_0. For diffusion, we introduce a diffusion microlayer with initial thickness δ_0 similar to the thermal microlayer with thickness d_0. It follows from the analogy between heat and diffusion, that:

$$\delta_{0,m} = \left(\frac{D}{a}\right)^{\frac{1}{2}} d_{0,p} \qquad \text{or} \qquad \delta_{0,m} = \left(\frac{D}{a}\right)^{\frac{1}{2}} \frac{C_{1,p}}{C_{1,m}} d_{0,m}, \tag{43}$$

whence

$$\frac{\delta_{0,m}}{d_{0,p}} = \frac{G_h^*}{G_d} = \left(\frac{D}{a}\right)^{\frac{1}{2}} \quad \text{or} \quad \frac{\delta_{0,m}}{d_{0,m}} = \left(\frac{D}{a}\right)^{\frac{1}{2}} \frac{C_{1,p}}{C_{1,m}} = \frac{G_h}{G_d}. \tag{44}$$

The material balance yields:

$$\left.\begin{aligned}(4\pi/3)\rho_2 R_1^3 y + A_i\rho_1\delta_m x &= A_i\rho_1\delta_{0,m}x_0 \\ G_d y + (1 - G_d)x &= x_0\end{aligned}\right\} \tag{45}$$

where $\delta_{0,m}$ and δ_m denote the thickness of the diffusion microlayer before and after vaporization respectively. Consequently:

$$G_d = \frac{(4\pi/3)\rho_2 R_1^3}{A_i\rho_1\delta_0} = \frac{\rho_2}{\rho_1}\vartheta_0\left(1 - \frac{1}{e}\right)C_{1,m}u_{1,m}\frac{1}{\delta_{0,m}}. \tag{46}$$

It follows from equations (30) and (31):

$$G_d = \left(\frac{a}{D}\right)^{\frac{1}{2}} \frac{C_{1,m}}{C_{1,p}} \frac{c}{l}\vartheta_0\left(1 - \frac{1}{e}\right),$$

which yields in combination with equation (46):

$$\delta_{0,m} = \frac{\rho_2}{\rho_1}\left(\frac{D}{a}\right)^{\frac{1}{2}} \frac{l}{c} C_{1,p}u_{1,p} = \left(\frac{12}{\pi}\right)^{\frac{1}{2}} D^{\frac{1}{2}}u_{1,p}, \tag{47}$$

independent of the composition of the mixture, whence in accordance with equation (35) of Part I of this paper

$$\delta_{0,m} = \left(\frac{D}{a}\right)^{\frac{1}{2}} d_{0,p}. \tag{48}$$

It is seen also from equation (46), that:

$$\delta_m = (1 - G_d)\delta_{0,m} = (1 - G_d)(12/\pi)^{\frac{1}{2}}D^{\frac{1}{2}}u_{1,p}$$

and the thickness of the vaporized microlayer

$$\delta_{0,m} - \delta_m = G_d\,(12/\pi)^{\frac{1}{2}}D^{\frac{1}{2}}u_{1,p} = G_h^*\,(12/\pi)^{\frac{1}{2}}a^{\frac{1}{2}}u_{1,p}. \tag{49}$$

For the investigated water–1-butanol and water–methylethylketone mixtures, $D^{\frac{1}{2}} = 3{\cdot}1 \times 10^{-5}$ m/s$^{\frac{1}{2}}$ at atmospheric boiling point, whence it follows from equation (47), that $\delta_{0,m} \approx 5$ μ, which is small in comparison to d_0; by taking the average value of G_d from Table 2, a microlayer with a thickness of approximately 1 μ is vaporized; this value agrees with the hypothetical layer assumed by Moore and Mesler [7]. The same value, of course, can also be obtained by considered the thermal microlayer with thickness $d_{0,m}$ (cf. Table 1 of Part I of this paper) and taking the corresponding value of G_h^* from Table 2. The thermal microlayer, which is periodically pushed away from the heating surface, contains a sufficiently large quantity of the more volatile component, as $\delta_0 \ll d_0$. This is the reason why the expression (21) of Part I of this paper for bubble growth at the heating surface, which is similar to $R = C_1\vartheta_0 t^{\frac{1}{2}}$ for free bubbles in an infinite liquid volume, is valid.

2.3 *Comparison with previous estimations of the vaporized fraction*

These were based on the assumption, that the growth of released vapour bubbles is reduced to

zero at the mole fraction $x_{0,M}$ of the more volatile component, in which a maximum increase ΔT in dew point occurs, if this quantity equals the superheating of the bulk liquid ([8–11] and the next Section):

$$\Delta T = - x_{0,M}(K_M - 1)\, G_{d,M}\, (\mathrm{d}T/\mathrm{d}x_M)_{x_M = x_{0,M}} = \Delta\vartheta_0. \tag{50}$$

The vaporized mole fraction $G_{d,M}$ could be determined graphically from this equation by making use of available equilibrium data. The values, which were obtained in this way, and those of the corresponding mass diffusion fraction G_d are shown in Table 2. Both are compared with the values calculated from equations (31) and (33) for bubbles generated at a highly superheated platinum wire. The recent values for free bubbles growing due to the liquid superheating $\Delta\vartheta_0$ only, are calculated from [6]:

$$G_d = (\rho_2/\rho_1)\varphi(\varepsilon, \mu\beta), \tag{51}$$

whence

$$G_d = 10{\cdot}4 C_{1,m}\Delta\vartheta_0$$

for water–1-butanol and water–methylethylketone mixtures.

The corresponding values of the mole fraction $G_{d,M}$ can be calculated from, [6]:

$$G_d = G_{d,M}\{1 + (M_1/M_2 - 1)y_M\}. \tag{52}$$

It is seen that the reason of the previously used values for free bubbles being rather satisfactory, is the good agreement with the recent values for bubbles growing at a heating surface.

Consequently, the important conclusion can be drawn, that the slowing down of bubble growth after release is not the most important factor which determines the occurrence of a maximum nucleate boiling peak flux density in binary mixtures, as was believed previously, but the reduced initial growth at the heating surface. This is in agreement with experimental results by Hovestreijdt [12] on water, which show that the peak flux in water is independent of the value of $\Delta\vartheta_0$.

2.4 *Graphical evaluation of the bubble growth constant in mixtures*

It is seen from equations (12) of Part I of this paper, and (31), that the expression for the bubble growth constant $C_{1,m}$ for free bubbles in uniformly superheated binary mixtures (e.g. subsequent growth of released bubbles due to the constant superheating of bulk liquid [6]) can be written:

$$C_{1,m} = \left(\frac{12}{\pi}\right)^{\frac{1}{2}} \frac{a^{\frac{1}{2}}}{\frac{\rho_2}{\rho_1}\left\{\frac{l}{c} + \left(\frac{a}{D}\right)^{\frac{1}{2}}\frac{\Delta T}{G_d}\right\}} = \left(\frac{12}{\pi}\right)^{\frac{1}{2}} \frac{a^{\frac{1}{2}}}{\frac{\rho_2}{\rho_1}\left(\frac{l}{c} + \frac{\Delta T}{G_h^*}\right)}. \tag{53}$$

One has thus, in combination with equations (32) and (30), respectively, for mixtures containing the less volatile component in excess, so that the values of the thermal quantities are changed insignificantly only:

$$C_{1,m} = \left(\frac{12}{\pi}\right)^{\frac{1}{2}} \frac{a^{\frac{1}{2}}}{\frac{\rho_2}{\rho_1}\left(\frac{l}{c} + \frac{C_{1,p}}{C_{1,m}}\frac{\Delta T}{G_h}\right)} = \left(\frac{12}{\pi}\right)^{\frac{1}{2}} \frac{a^{\frac{1}{2}}}{\frac{\rho_2 l}{\rho_1 c}\left(1 + \frac{\mathrm{e}}{\mathrm{e}-1}\frac{C_{1,p}}{C_{1,m}}\frac{\Delta T}{\vartheta_0}\right)}$$

$$= \frac{C_{1,p}}{1 + \frac{\mathrm{e}}{\mathrm{e}-1}\frac{C_{1,p}}{C_{1,m}}\frac{\Delta T}{\vartheta_0}},$$

i.e. the expression for $C_{1,m}$ simplifies to:

$$\frac{C_{1,m}}{C_{1,p}} = 1 - \frac{e}{e-1}\frac{\Delta T}{\vartheta_0} = 1 - 1{\cdot}58\frac{\Delta T}{\vartheta_0}. \tag{54}$$

It is essential that $\Delta T/G_d$ is—according to equation (50)—independent of G_d, hence $\Delta T/G_h^*$, $\Delta T/G_h$ and $\Delta T/\vartheta_0$ are also independent of G_h^*, G_h and ϑ_0, respectively, i.e. ΔT is proportional to ϑ_0. A maximum ΔT occurs (at constant ϑ_0) at 4·1 wt. % ($x_0 = 4{\cdot}1 \times 10^{-2}$) methylethylketone in the binary system water–methylethylketone, and at 1·5 wt. % ($x_0 = 1{\cdot}5 \times 10^{-2}$) 1-butanol in water–1-butanol. The atmospheric boiling points of these mixtures are decreased in comparison to water with 11·5 degC and 2·6 degC, respectively. The vaporized fraction $G_d = (x_0 - x)/(y - x) = (x_0 - x)/(K - 1)x$ is relatively large for bubbles generated at a heating surface (order of magnitude 10^{-1}, cf. the more accurate values in Table 2) despite the large value of the equilibrium constant $K = y/x$ (16·5 and 17·5, respectively). Roughly speaking, one can thus take $x = 0$, i.e. the more volatile component is completely exhausted at the bubble boundary, and the dew temperature of the vapour in the bubble space is 100·0 degC, whence $\Delta T = 11{\cdot}5$ degC and 2·6 degC for $\vartheta_0 = 24$ degC and 21 degC, respectively.

It follows by substitution of these values in equation (54), that $C_{1,m} = 5{\cdot}8 \times 10^{-4}$ m/s$^{\frac{1}{2}}$ degC for 4·1 wt. % methylethylketone and $C_{1,m} = 19 \times 10^{-4}$ m/s$^{\frac{1}{2}}$ degC for 1·5 % 1-butanol as $C_{1,p} = 24 \times 10^{-4}$ m/s$^{\frac{1}{2}}$ degC for water. These estimated values approximate the experimental and exact theoretical values closely (6×10^{-4} and 18×10^{-4} m/s$^{\frac{1}{2}}$ degC, respectively, [6] and Table 2). Also, the important conclusion can be drawn that the assumption concerning the dew temperature of the vapour in the bubble, which should equal the value at the liquid-level surface, must be correct. This dew temperature in the bubble space has at present not yet been measured experimentally.

The azeotropic boiling point in the binary system water–1-octanol is only slightly (0·6 degC) below that of water. Consequently, $\Delta T \leqslant 0{\cdot}6$ degC regardless of the value of ϑ_0; i.e. in spite of the very high relative volatility of 1-octanol here, which exceeds the values of the lower aliphatic alcohols considerably, bubble growth will not be affected appreciably, whence the increase in peak flux is only small, the more so as the more volatile component is rapidly exhausted in the liquid at the heating surface. This prediction is in agreement with previous experimental results [9, 8, 11], cf. also the effect of trace additives on the heat transfer to boiling iso-propanol by Dunskus and Westwater [13].

One can easily derive from equation (12) of Part I of this paper the ratio of the growth constants:

$$\frac{C_{1,p}}{C_{1,m}} = 1 + \left(\frac{a}{D}\right)^{\frac{1}{2}} \frac{c}{l}\frac{\Delta T}{G_d}.$$

This equation is most suitable for obtaining $C_{1,m}$ graphically in dependence on liquid composition, as $\Delta T/G_d$ follows directly from equilibrium data (i.e. the experimental boiling point curve $T(x)$ and the corresponding dew-point curve $T(y)$ at constant ambient pressure), according to van Wijk and van Stralen [14, 8, 11].

One can also derive $\Delta T(x_0)/G_d$ from the approximation:

$$\frac{\Delta T(x_0)}{G_d} = -x_0\{K(x) - 1\}\left(\frac{dT}{dx}\right)_{x=x_0} \approx -x_0\{K(x_0) - 1\}\left(\frac{dT}{dx}\right)_{x=x_0},$$

which is the fundamental basis of the graphical method, cf. [8].

It is possible now to obtain previous information about the suitability of a binary system with

respect to peak flux behaviour, since both $C_{1,m}$ and the concentration of maximal ΔT are determined from the same graph. This procedure can save a lot of insignificant experimental work, Figs. 2 and 3.

In addition, it may be worth reporting, that previously [8, 11] a value of the bubble growth constant in binary mixtures has been used, which is nearly identical to equation (54), viz.:

$$\frac{C_{1,m}}{C_{1,p}} = 1 - \frac{\Delta T}{\vartheta_0},$$

whence $C_{1,m}$ shows a minimum at the concentration of maximum ΔT; the value of this minimum is reduced to zero, by taking the vaporized fraction such that the maximal $\Delta T = \vartheta_0$.

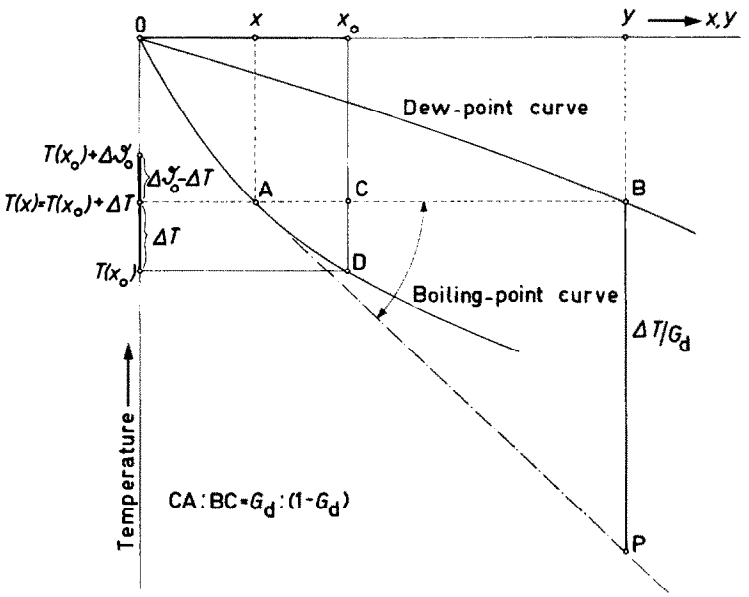

FIG. 2. Equilibrium diagram for binary system with minimum boiling point. One has: $(x_0 - x)/(y - x_0) = G_d/(1 - G_d)$, which equation is for small values of G_d simplified to $(y - x)/(x_0 - x) = 1/G_d$, whence BP = (BA/CA)CD = Δ/G_d, independent of G_d.
$\Delta\vartheta_0$ has been used here instead of ϑ_0.

Consequently, it has been shown here, that the basis of this equation, which was derived already before theoretical solutions of the linked heat and mass diffusion equations were known, still holds: the slowing down of bubble growth in certain binary mixtures is due to the reduction of the superheating ϑ_0 of the pure solvent to the "effective" value $\vartheta_0 - \Delta T$, i.e. the superheating in mixtures has been lowered due to the increase ΔT in dew temperature of saturated vapour in the bubble.

3. THE MAXIMUM NUMBER OF ACTIVE NUCLEI GENERATING VAPOUR BUBBLES IN NUCLEATE BOILING

3.1 *Geometrical analysis*

The surface area of the cylinder, which is coaxial with a (horizontal) heating wire, and of which

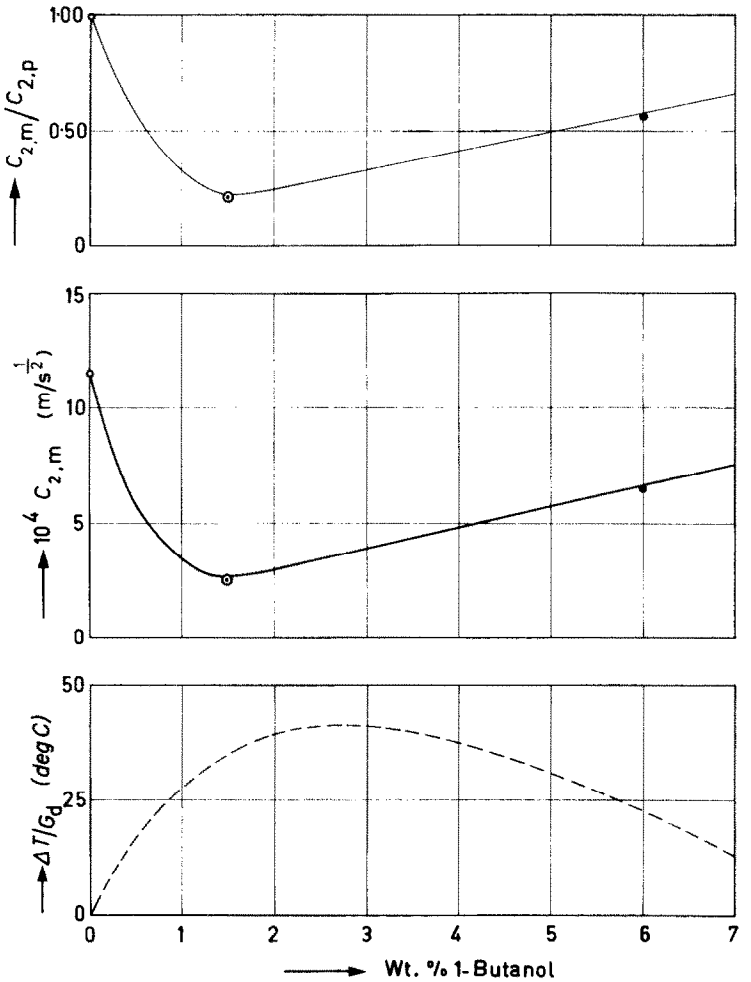

FIG. 3. *Water–1-butanol.* Experimental (○, ⊙, ●) and theoretical (curves) values of $C_{2,m}$ and the ratio $C_{2,m}/C_{2,p}$ according to exact bubble growth equation [6]: $\Delta T/G_d = -x_0(K-1)(dT/dx)_{x=x_0} = \{\Delta\vartheta_0 - (\rho_2 l/\rho_1 c)\varphi(\epsilon,\beta)\}/\{(\rho_2/\rho_1)\varphi(\epsilon,\mu\beta)\}$ for released bubbles, at actually measured superheating of bulk liquid $\Delta\vartheta_0 = 0{\cdot}36$ deg C in water, 0·14 deg C in 1·5% and 0·31 deg C in 6·0 wt. % 1-butanol.

The $\Delta T/G_d$-curve was obtained graphically from equilibrium data, cf. Fig. 2. The concentration of maximum $\Delta T/G_d$ exceeds the concentration of minimum $C_{2,m}$ slightly due to the dependence of the latent heat of vaporization on composition.

Experimental results and theoretical predictions are in quantitative agreement.

the radius z equals the distance of the axis to the centre of the spherical vapour bubble, amounts to (Fig. 4):

$$2\pi L_w z = 2\pi L_w \{\tfrac{1}{2}D_w + (2B - 1)R_1^*\}. \tag{55}$$

The area of intersection with a vapour bubble at the instant of departure can be approximated by $\pi(R_1^*)^2$.

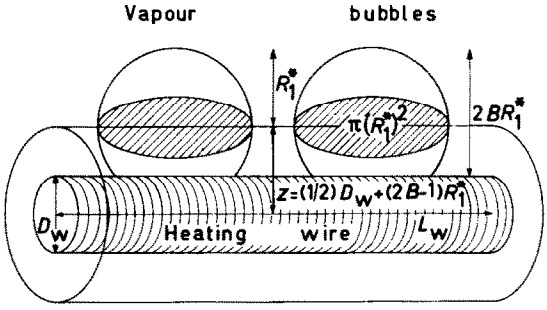

FIG. 4. Simultaneous departure of vapour bubbles from horizontal heating wire with circular cross-section.

One can derive now a new criterion for the maximum number of nuclei per unit area of heating surface for bubble formation on the wire, which are activated before the onset of film boiling occurs: the entire surface area of this cylinder is covered with touching vapour bubbles. Consequently:

$$m_{\max} = \frac{2\pi L_w\{\tfrac{1}{2}D_w + (2B - 1)R_1^*\}}{\pi(R_1^*)^2}, \tag{56}$$

whence the maximal density of active nuclei is given by the expression:

$$\frac{m_{\max}}{A_w} = \frac{2\pi L_w\{\tfrac{1}{2}D_w + (2B - 1)R_1^*\}}{\pi(R_1^*)^2\pi D_w L_w} = \frac{D_w + 2(2B - 1)R_1^*}{\pi D_w(R_1^*)^2}. \tag{57}$$

The right-hand side of equation (57) is independent of the wire length L_w, as should be. One can use for $D_w \ll R_1^*$ the approximation:

$$\frac{m_{\max}}{A_w} = 2\frac{2B - 1}{\pi D_w R_1^*}. \tag{58}$$

It follows from equation (57), for water boiling at peak flux conditions on a platinum wire with a diameter $D_w = 2 \times 10^{-4}$m, $\overline{R}_1 = 9{\cdot}2 \times 10^{-4}$m and thus $\overline{R_1^*} = (\frac{32}{7})^{\frac{1}{3}}\overline{R}_1 = 1{\cdot}06\overline{R}_1 = 9{\cdot}75 \times 10^{-4}$m, as B = 0·75 (Part I of this paper): $m_{\max}/A_w = 1{\cdot}99 \times 10^6$ nuclei/m^2, (see Table 3). For 4·1 wt. % methylethylketone $\overline{R}_1 = 3{\cdot}4 \times 10^{-4}$m and thus $\overline{R_1^*} = 3{\cdot}6 \times 10^{-4}$m, as $B = 0{\cdot}75$, whence $m_{\max}/A_w = 6{\cdot}84 \times 10^6$ nuclei/m^2.

For very thin heating wires, it may be of importance to predict the effect of wire diameter on peak flux. It is seen from equation (58), that $m_{\max}/A_w$ is increasing for decreasing D_w, if a constant R_1^* is assumed. It follows, that $m_{\max}/A_w$ is inversely proportional with D_w^2, if R_1^* is assumed to be

proportional with D_w. Hence, in both cases $m_{max}/A_w \to \infty$ as $D_w \to 0$. As $D_w \to \infty$ (large heaters), it is seen from equation (57), that

$$\frac{m_{max}}{A_w} \to \frac{1}{\pi (R_1^*)^2}. \tag{59}$$

3.2 *Nucleation theory*

It has been shown previously [8, 11], both for water and for 4·1 wt. % methylethylketone, boiling on horizontal platinum wires under atmospheric pressure, that in the region of nucleate boiling one can use the empirical expression for common "physically pure" (99·99 %) wires:

$$\frac{m}{A_w} = \frac{1}{\pi D_w l_w} [\exp \{0{\cdot}27 (\vartheta_0 - \vartheta_1)\} - 1], \tag{60}$$

an expression, which has the same shape as predicted by the homogeneous nucleation theory, cf. [15, 16], as (D_4 = Boltzmann constant = $1{\cdot}38 \times 10^{-23}$ J/degK):

$$\frac{\exp \{-W/D_4(T + \vartheta_0)\}}{\exp \{-W/D_4(T + \vartheta_1)\}} = \exp \{W(\vartheta_0 - \vartheta_1)/D_4 T^2\}, \tag{61}$$

provided that $\vartheta_0 \ll T$, whence the condition $\vartheta_1 \ll T$ is also satisfied.

For water $m_{max}/A = 1{\cdot}20 \times 10^6$ nuclei/m^2 is predicted as $\vartheta_0 - \vartheta_1 = 13{\cdot}5$ degC, and for 4·1 wt. % methylethylketone $m_{max}/A_w = 7{\cdot}10 \times 10^6$ nuclei/m^2, as $\vartheta_0 - \vartheta_1 = 20$ degC, Table 3. It may be noticed here, that $T + \vartheta_{0,max} = 122$ degC for both liquids, viz. (100 + 21·5) degC for water and (88·5 + 34) degC for the mixture, whence the maximum of nucleate boiling is reached at the same, "critical", wire temperature [8, 11], (second criterion for the onset of film boiling).

3.3 *Present theory*

It has been shown here, Section 1.3, that the area of influence of a vapour bubble at the heating surface, amounts to:

$$A_i = \frac{4\pi}{3(e - 1)} b R_1^2. \tag{62}$$

It is assumed, that the maximum nucleate boiling heat flux density occurs, if the entire heating surface is covered with bubble microlayers of area A_i (third criterion for the onset of film boiling, which is independent of the shape of the heating surface).

For water

$$A_i = 1{\cdot}71\, R_1^2 \qquad \text{and} \qquad \bar{R}_1 = 9{\cdot}2 \times 10^{-4} \text{ m},$$

whence $m_{max}/A_w = 0{\cdot}70 \times 10^6$ nuclei/m^2 (experimental value $1{\cdot}13 \times 10^6$ nuclei/m^2), for 4·1 wt. % methylethylketone $A_i = 2{\cdot}20\, R_1^2$ and $\bar{R}_1 = 3{\cdot}4 \times 10^{-4}$ m, whence $m_{max}/A_w = 3{\cdot}95 \times 10^6$ nuclei/m^2, cf. Table 3.

One has thus:

$$m_{max} A_i = A_w \tag{63}$$

or

$$\frac{m_{max}}{A_w} = \frac{1}{A_i} = \frac{3(e - 1)}{4\pi b R_1^2}. \tag{64}$$

Equation (64) predicts for flat heating plates an 80 per cent higher maximal density of active nuclei (if $b = 0{\cdot}80$ has been taken) in comparison with equation (59).

4. THE MAXIMUM NUCLEATE BOILING HEAT FLUX DENSITY ("PEAK FLUX")

4.1 *Pure liquids*

The contribution to the peak flux of the direct vapour formation at the heating surface amounts to, cf. equations (64), (18) and (30):

$$q_{w,b,\max} = \frac{m_{\max}}{A_w}\frac{4\pi}{3}\rho_2 l R_1^3 v = \frac{1}{A_i} A_i \rho_2 l C_1 u_1 \vartheta_{0,\max}\left(1 - \frac{1}{e}\right) v$$

$$= \rho_2 l C_1 u_1 \vartheta_{0,\max}\left(1 - \frac{1}{e}\right) v = \frac{\rho_2 l^2}{c} C_1 u_1 v G_{h,\max}, \qquad (65)$$

i.e. $q_{w,b,\max}$ is independent of A_i. Equation (65) enables us to determine the enthalpy of the direct vapour formation from the vaporized mass fraction.

It follows that:

$$q_{w,b,\max} = \rho_2 l \left\{\left(\frac{12}{\pi}\right)^{\frac{1}{2}} \frac{a^{\frac{1}{2}}}{\rho_2 l}\rho_1 c\right\} u_1 \vartheta_{0,\max}\left(1 - \frac{1}{e}\right)\frac{1}{4u_1^2}$$

$$= \tfrac{1}{2}\left(\frac{3}{\pi}\right)^{\frac{1}{2}}\left(\frac{a}{t_1}\right)^{\frac{1}{2}} \rho_1 c \vartheta_{0,\max}\left(1 - \frac{1}{e}\right) = \tfrac{1}{2}\left(\frac{3}{\pi}\right)^{\frac{1}{2}}\left(\frac{a}{t_1}\right)^{\frac{1}{2}} \rho_1 l G_{h,\max}, \qquad (66)$$

where according to equation (30):

$$G_{h,\max} = \frac{c}{l}\vartheta_{0,\max}\left(1 - \frac{1}{e}\right). \qquad (67)$$

One has for water:

$$q_{w,b,\max} = 15{\cdot}9 \times 10^4 \text{ W/m}^2$$

by taking $t_1^{\frac{1}{2}} = 7 \times 10^{-2}\, s^{\frac{1}{2}}$ and $G_{h,\max} = (\vartheta_{0,\max}/20)\, 23{\cdot}6 \times 10^{-3}$, cf. Table 2, with $\vartheta_{0,\max} = 21{\cdot}5$ degC. This value is considerably too low, since actually $v = 1/2{\cdot}76 t_1$ instead of $v = \frac{1}{4}t_1$ (Table 1) and $m_{\max}/A_w = 1{\cdot}13 \times 10^6$ nuclei/m^2, Table 3, instead of $1/A_i = 0{\cdot}70 \times 10^6$ nuclei/m^2. The more correct value is thus: $q_{w,b,\max} = 37{\cdot}2 \times 10^4$ W/m^2, whence the theoretical peak flux amounts to:

$$q_{w,\max} = q_{w,co,\max} + q_{w,b,\max} = (33{\cdot}1 + 37{\cdot}2)\, 10^4 \text{ W/m}^2 = 70 \times 10^4 \text{W/m}^2, \qquad (68)$$

in quantitative agreement with the experimental value (67×10^4 W/m^2).

4.2 *Binary mixtures*

One has for mixtures with small values of the bubble growth constant $C_{1,m}$ the approximation:

$$q_{w,b,\max} = \frac{\rho_2 l^2}{c} C_{1,m} u_{1,m} v G_{h,\max} = \frac{\rho_2 l^2}{c} C_{1,m} u_{1,p} G_{h,\max}\frac{1}{u_{1,p}^2}$$

$$= \frac{\rho_2 l^2}{c u_{1,p}} C_{1,m} G_{h,\max} = \frac{\rho_2 l^2}{c u_{1,p}} C_{1,p} G^*_{h,\max}. \qquad (69)$$

Obviously, one has for these mixtures at arbitrary constant ϑ_0 in nucleate boiling:

$$q_{w,b,m} = \frac{C_{1,m}}{C_{1,p}} \frac{\rho_2 l^2}{c u_{1,p}} C_{1,p} G_{h,m} = 4 \frac{C_{1,m}}{C_{1,p}} \frac{\rho_2 l^2}{4 c u_{1,p}} C_{1,p} G_{h,p} = 4 \frac{C_{1,m}}{C_{1,p}} q_{w,b,p},$$

whence $q_{w,b,m} = q_{w,b,p}$ for 4·1 wt. % methylethylketone in comparison with water. From equation (69), for 4·1 wt. % methylethylketone in water, one finds a value of $q_{w,b,\max} = 24{\cdot}7 \times 10^4$ W/m^2, see Tables 2 and 3. A very interesting advantage of making use of the vaporized fraction is, that the whole increase in peak flux above convection, $q_{w,bi,\max} = q_{w,\max} - q_{w,co,\max}$, which is ultimately caused by the bubble formation, can now also be calculated directly.

For pure liquids one has:

$$q_{w,bi} = q_w - q_{w,co} = q_{w,b} \tag{70}$$

on account of the definition of the microlayer thickness. Contrarily, in binary mixtures:

$$q_{w,bi} = q_w - q_{w,co} \geqslant q_{w,b}, \tag{71}$$

or more exactly at the peak flux:

$$q_{w,bi,\max} = q_{w,\max} - q_{w,co,\max} = \frac{\rho_2 l^2}{c u_{1,p}} C_{1,p} G_{h,\max} = \frac{C_{1,p}}{C_{1,m}} q_{w,b,\max}. \tag{72}$$

Hence, in our example $q_{w,bi,\max} = 4 \times 24{\cdot}7 \times 10^4$ W/m^2 $= 99 \times 10^4$ W/m^2, a value which must be increased, see Table 3 and Section 4.3 on account of the actually higher $m_{\max}$. This is resulting in a too low theoretical peak flux.

4.3 *General method*

An even more elegant way to solve the problem of derivation of the peak flux theoretically is obtained by writing for mixtures:

$$q_{w,b,\max} = \frac{m_{\max}}{A_w} \frac{4\pi}{3} \rho_2 l R_1^3 \nu = \frac{1}{A_i} A_i \rho_1 c d_{0,m} \vartheta_{0,\max} \left(1 - \frac{1}{e}\right) \nu$$

$$= \rho_1 c d_{0,m} \vartheta_{0,\max} \left(1 - \frac{1}{e}\right) \nu = \rho_1 c d_{0,m} \frac{l}{c} G_{h,\max} \nu = \rho_1 l d_{0,m} G_{h,\max} \nu = \rho_1 l d_{0,p} G^*_{h,\max} \nu, \tag{73}$$

an expression which is simplified for pure liquids, in which $G^*_{h,\max} = G_{h,\max}$. For water, $d_0 = 63{\cdot}3$ μ (Table 1 of Part I of this paper), $G_{h,\max} = (21{\cdot}5/20)23{\cdot}6 \times 10^{-3}$ (Table 2), whence $q_{w,b,\max} = 30{\cdot}2 \times 10^4$ W/m^2 by taking the average value $\bar{\nu}_e = 70$ 1/s following from the average $\overline{t^{\frac{1}{2}}_{1,e}} = 7{\cdot}0 \times 10^{-2}$ s$^{\frac{1}{2}}$ and from $\nu_e = 1/2{\cdot}76\, t_{1,e}$, Table 1, or from the product $(4\pi/3)\rho_2 l \overline{\nu R_1^3}$ in Table 1 (37×10^4 W/m^2) and from the average $\bar{R}_1 = 9{\cdot}2 \times 10^{-4}$ m (Table 3), which follows from $R_1 = (b/e)\, C_{1,p} \vartheta_{0,\max} t^{\frac{1}{2}}_1$. For 4·1 wt. % methylethylketone, the average $\bar{\nu}_e = 175$ 1/s (Table 3, from (3·00/1·19)70 1/s, cf. Table 1), whence it follows from the value in water: $q_{w,bi,\max} = 30{\cdot}2 \times 10^4 (34/21{\cdot}5)(175/70)$ W/m^2 $= 120 \times 10^4$ W/m^2 and $q_{w,b,\max} = (C_{1,m}/C_{1,p}) q_{w,bi,\max} = (\frac{1}{4}) 120 \times 10^4$ W/m^2 $= 30 \times 10^4$ W/m^2. This results in a theoretical peak flux $q_{w,\max} = 171 \times 10^4$ W/m^2, also in quantitative agreement with the experimental value (172×10^4 W/m^2), cf. Fig. 1 of Part I of this paper.

It is shown here, that the maximum direct vapour formation $q_{w,b,\max}$ is practically independent of the composition of the mixture. This yields a fourth criterion for the onset of film boiling, cf. Section 3.

In general, one has to consider that the total increase in heat flux density due to bubbles in mixtures throughout the region of nucleate boiling is given by the expression:

$$q_{w,bi} = q_w - q_{w,co} = \rho_1 l d_{0,p} G_h v_m \tag{74}$$

and the direct vapour formation at the heating surface by:

$$q_{w,b} = \rho_1 l d_{0,m} G_h v_m, \tag{75}$$

whence $q_{w,bi} = q_{w,b}$ in pure liquids, in contrast to mixtures, where

$$\frac{q_{w,b}}{q_{w,bi}} = \frac{d_{0,m}}{d_{0,p}} \approx \frac{C_{1,m}}{C_{1,p}} \leqslant 1. \tag{76}$$

The occurrence of high peak flux values in mixtures at the same low concentration of the more volatile component of maximal slowing down of bubble growth rates (minimum C_1, cf. also Fig. 3 of Part I of this paper) is due to a combination of a considerably higher bubble frequency and an increased maximal superheating $\vartheta_{0,m,\max} = \vartheta_{0,p,\max} + T_p - T_m$.

4.4 *Bubbles on complex nuclei in water–1-butanol mixtures*

In 1·5 wt. % 1-butanol, where nearly all ordinary nuclei have been replaced by complex nuclei at the peak flux, one has (cf. the Appendix and Table 1)

$$\frac{v_c}{v_p} = \frac{2(1/2{\cdot}69 t_{1,p})}{\frac{1}{4} t_{1,p}} = 3{\cdot}0,$$

whence the theoretical peak flux amounts to $30{\cdot}2 \times 10^4 \times 3{\cdot}0 \times (27{\cdot}5/21{\cdot}5) + 41{\cdot}5 \times 10^4$ W/m^2 = 157×10^4 W/m^2 in good agreement with the experimental value (169×10^4 W/m^2).

In 6·0 wt. % 1-butanol $v_c/v_p = 8/3{\cdot}3 = 2{\cdot}4$ and $q_{w,\max} = 133 \times 10^{-3}$ W/m^2 (experimental value: 126×10^4 W/m^2, cf. Fig. 2 of Part I of this paper and Table 3.

4.5 *Conclusions*

The present theory predicts the previously observed coincidence of maximum peak flux density in nucleate boiling and minimum bubble growth rates at the same (low) concentration of the more volatile component in binary systems. It has been shown previously that this concentration can be deduced from equilibrium data [8–11, 14], cf. Section 2·4.

Quantitative agreement with experimental data exists in the binary systems investigated both for peak flux and bubble growth. A higher peak flux in mixtures corresponds with a smaller direct vaporization rate at the heating surface. The entire excess enthalpy of the thermal boundary layer at the surface is required for vaporization at the wall in pure liquids, in contrast to the behaviour in mixtures, where the main part of the excess enthalpy is transmitted to the adjacent colder bulk liquid.

In principle, the theoretical predictions include the favourable effect on peak flux by all other methods resulting in a diminished vapour production at the heating surface (which corresponds generally with an increased frequency of smaller bubbles), e.g. surface boiling, vortex flow, the use of high pressures and the application of an electrostatic field.

4.6 *Comparison with the Zuber and Tribus theory*

A necessary condition for the stability of film boiling is the occurrence of a standing capillary

wave, according to Zuber [18] and Zuber and Tribus [19]. The wavelength at the minimum heat flux density (i.e. at the Leidenfrost-point between transition boiling and film boiling) is given by:

$$\lambda = 2\pi\left\{\frac{\sigma}{g(\rho_1 - \rho_2)}\right\}^{\frac{1}{2}}. \tag{77}$$

Unfortunately, Zuber's theory fails to indicate how the first waves originate by gradually increasing superheating at the transition from the region of nucleate boiling to the region of transition boiling. This, however, is obvious from the present theory: the oscillating thermal microlayer (in pure liquids, for convenience) is similar to a propagation of waves with the velocity

$$v = \nu\lambda = \frac{1}{t_1 + t_2} 4R_i = \frac{4R_i}{4t_1} = \frac{R_i}{t_1}, \tag{78}$$

where the radius R_i of the region of influence of a bubble follows from:

$$A_i = \frac{4\pi}{3(\mathrm{e} - 1)} bR_1^2 = \pi R_i^2 \tag{79}$$

or

$$R_i = 2\left\{\frac{b}{3(\mathrm{e} - 1)}\right\}^{\frac{1}{2}} R_1. \tag{80}$$

Hence,

$$v = \frac{2b}{\mathrm{e}u_1} C_{1,p}\,\vartheta_0 \left\{\frac{b}{3(\mathrm{e} - 1)}\right\}^{\frac{1}{2}}, \tag{81}$$

with

$$C_{1,p} = \left(\frac{12}{\pi}\right)^{\frac{1}{2}} \frac{\rho_1 c}{\rho_2 l} a^{\frac{1}{2}}. \tag{82}$$

Thus

$$\lambda = 4R_i = 4t_1 v = 16\left(\frac{3}{\pi}\right)^{\frac{1}{2}} \frac{b}{\mathrm{e}} \left\{\frac{b}{3(\mathrm{e} - 1)}\right\}^{\frac{1}{2}} \frac{\rho_1 c}{\rho_2 l} a^{\frac{1}{2}} \vartheta_0 u_1 \tag{83}$$

e.g. for bubbles in water, one has $\lambda = 16 \times 10^{-5}\,\vartheta_0$. This equals the wavelength at the Leidenfrost-point from equation (77): $\lambda = 1{\cdot}54 \times 10^{-2}$ m for $\vartheta_0 = 100$ degC, which is in good agreement with experiments, cf. Fritz's data [20]. For ethanol, $C_1 = 9 \times 10^{-4}$ m/s$^{\frac{1}{2}}$ degC, whence $\lambda = 4{\cdot}7 \times 10^{-5}\,\vartheta_0$ must be compared with $0{\cdot}94 \times 10^{-2}$ m; $\vartheta_0 = 200$ degC is found in agreement with a relatively high superheating at the nucleate boiling peak flux. For 4·1 wt. % methylethylketone $t_2 \ll t_1$, and $\lambda = 4R_i \approx t_1 v = 3{\cdot}3 \times 10^{-5}\,\vartheta_0$ must equal $1{\cdot}30 \times 10^{-2}$ m, whence the occurrence of the Leidenfrost-point is predicted at the high superheating $\vartheta_0 = 400$ degC. Unfortunately, experimental data on this subject are hitherto completely lacking in literature.

4.7 *Survey*

The general procedure of obtaining the behaviour of adhering bubbles in binary mixtures including pure liquids, can be summarized as follows:

(i) d_w is determined from the lower part of the boiling curve, or from convection equations for free, forced or combined convection.

(ii) $d_{0,p}$, which is for practical purposes a quantity of minor importance, is calculated by means of equation (28).
(iii) The corresponding quantity $d_{0,m}$ follows then from $d_{0,p}$ by multiplying with $C_{1,m}/C_{1,p}$, i.e. the ratio of the bubble growth constants.
(iv) t_1 from equation (34) of Part I of this paper.
(v) $R(t)$ and R_1 from equations (21) and (45) of Part I, respectively.
(vi) t_2 and v from equations (9) and (16), respectively.
(vii) m_{max}/A_w from equation (64).
(viii) G_h^* from equations (32) and (30).
(ix) The nucleate boiling peak flux density from equation (73).

Manipulation (iii) is cancelled and (vi) and (viii) are simplified for pure liquids.

It may be worth reporting, that the convection contribution to the peak flux is considered here to be independent of the bubble induced heat flux. This can, more formally, also be treated theoretically by increasing $q_{w,i}$ in equation (11) with a separate convection term or by a multiplication factor depending on the average liquid velocity [17].

The convective heat flux in pure liquids is partly used for subsequent bubble growth after release, which is associated with a uniform superheating $\Delta\vartheta_0$ of the bulk liquid, and for the rest for an increased evaporation rate at the liquid-level surface, which is disturbed continuously due to bubble agitation. It may be possible to derive $\Delta\vartheta_0$ from the energy balance. Obviously, an increased roughness of the heating surface promotes nucleation and results in a decrease of $\Delta\vartheta_0$ cf. [1–3].

That part of the excess enthalpy of the pulsating relaxation microlayer in binary mixtures, which remains after subtraction of the direct vapour formation, is in first instance transferred to the surrounding bulk liquid and afterwards also used for subsequent bubble growth after release. The growth rate of individual bubbles at the heating surface is diminished in comparison with the behaviour in the pure, less volatile component, but this decrease is apparently of minor importance with respect to the larger bubble population and the smaller ascending velocity.

An eventual influence, if any, of surface tension σ on the delay time is left out of consideration. If this effect, which can appear in connection with nucleation only, should be observed actually, the theoretical value of t_2 must be shortened for decreasing σ, cf. equation (43) of Part I of this paper. It is believed, however, that this effect is incorporated already in the relaxation criterion for the superheating of the pulsating boundary layer.

REFERENCES

1. S. J. D. VAN STRALEN, The mechanism of nucleate boiling in pure liquids and in binary mixtures, Part I, *Int. J. Heat Mass Transfer* **9**, 995–1020 (1966).
2. M. JAKOB, Heat transfer in evaporation and condensation, *Mech. Engng* **58**, 643–660, 729–739 (1936).
3. M. JAKOB, *Heat Transfer*, Vol. 1. John Wiley, New York (1950).
4. C. J. RALLIS and H. H. JAWUREK, Latent heat transport in saturated nucleate boiling, *Int. J. Heat Mass Transfer* **7**, 1051–1068 (1964).
5. H. S. CARSLAW and J. C. JAEGER, *Conduction of Heat in Solids*, 2nd edn. Oxford Univ. Press, Oxford (1959).
6. S. J. D. VAN STRALEN, The growth rate of vapour bubbles in superheated pure liquids and in binary mixtures, Parts I–IV, accepted for publication in *Br. Chem. Engng* **11** (1966); **12** (1967).
7. F. D. MOORE and R. B. MESLER, The measurement of rapid surface temperature fluctuations during nucleate boiling of water, *A.I.Ch.E. Jl* **7**, 620–624 (1961).
8. S. J. D. VAN STRALEN, Warmteoverdracht aan kokende binaire vloeistofmengsels, Doctor thesis, Univ. of Groningen, Netherlands; Veenman, Wageningen, Netherlands (1959); *Meded. Landbhoogesch. Wageningen* **59** (6), 1 (1959). In Dutch with English summary and captions.
9. W. R. VAN WIJK, A. S. VOS and S. J. D. VAN STRALEN, Heat transfer to boiling binary liquid mixtures, *Chem. Engng Sci.* **5**, 68–80 (1956).

10. W. R. VAN WIJK, Wärmeübertragung an siedenden Zweistoffgemischen, *Dechema-Monogr.* **28**, 63–74 (1965).
11. S. J. D. VAN STRALEN, Heat transfer to boiling binary liquid mixtures, *Br. Chem.Engng* **4**, 8–17 (1959); **4**, 78–82 (1959); **6**, 834–840 (1961); **7**, 90–97 (1962).
12. J. HOVESTREIJDT, The influence of the surface tension difference on the boiling of mixtures, *Chem. Engng Sci.* **18**, 631–639 (1963).
13. T. DUNSKUS and J. W. WESTWATER, The effect of trace additives on the heat transfer to boiling isopropanol, *Chem. Engng. Prog. Symp. Ser.* 32. **57**, 173–180 (1961).
14. W. R. VAN WIJK and S. J. D. VAN STRALEN, Wärmeübertragung an siedenden Zweistoffgemischen II, *Dechema-Monogr.* **32**, 94–106 (1959).
15. M. VOLMER, *Kinetik der Phasenbildung*, Steinkopff, Dresden/Leipzig (1939).
16. J. W. WESTWATER, Boiling of liquids, in *Advances in Chemical Engineering*, Vols. 1, 2. Academic Press, New York (1956, 1958).
17. J. L. HUDSON and S. G. BANKOFF, An exact solution of unsteady heat transfer to a shear flow, *Chem. Engng Sci.* **19**, 591–598 (1964).
18. N. ZUBER, On the stability of boiling heat transfer, *Trans. Am. Soc. Mech. Engrs* **80**, 711–720 (1958).
19. N. ZUBER and M. TRIBUS, Further remarks on the stability of boiling heat transfer, Rep. 58-5, Dept. of Engng, Univ. of California, Los Angeles (1958).
20. W. FRITZ, Grundlagen der Wärmeübertragung beim Verdampfen von Flüssigkeiten, *Chemie-Ingr-Tech.* **35**, 753–764 (1963).

APPENDIX

Data concerning the departure size, the adherence and delay times, the frequency, etc., for bubbles generated on a horizontal platinum heating wire at a moderate constant heat flux density $q_w = 45 \times 10^4$ W/m^2 in nucleate boiling are shown in Table 1. The contribution to q_w of the direct vapour formation at the heating surface is given by $q_{w,b} = (4\pi/3)(m/A_w)\rho_2 l\overline{\nu R_1^3}$, and the convection contribution by $q_{w,co} = 1{\cdot}49 \times 10^4\ \vartheta_0$, cf. Fig. 1 of Part I of this paper, and [11].

Comparison of average experimental results with theory

t_2/t_1; *water*. 3·00 > 1 (theor.) and 1·76 (exp. for bubbles with $\nu = 50\ s^{-1}$); the deviation from the theory is due to the use of a.c. heating, the correct value using d.c. should be $\nu = 29{\cdot}3\ s^{-1}$.

4·1 wt. % *methylethylketone*. 0·19 < 1 (theor.) and 0·48 (exp., with exception of two bubbles with larger delay times apparently also due to a.c. heating as bubbles cannot originate at an instant of zero heating).

1·5 wt. % 1-*butanol*. 1·69 (theor.) and 2·00 (exp.). A lower $t_{2,e}/t_{1,e}$ may be expected than the theoretical value 3·00 for pure liquids, since it follows from the occurrence of local temperature dips that cold liquid is rushing to the heating surface already before bubble departure, see Part I of this paper.

νR_1^2; *water*. $4{\cdot}04 \times 10^{-5}$ (theor.) and $6{\cdot}40 \times 10^{-5}$ (exp., should be $3{\cdot}75 \times 10^{-5}$ for $\nu = 29{\cdot}3\ s^{-1}$).

4·1 wt. % *methylethylketone*. $1{\cdot}25 \times 10^{-5}$ (theor.) and $1{\cdot}31 \times 10^{-5}$ (exp.).

1·5 wt. % 1-*butanol*. $3{\cdot}83 \times 10^{-5}$ (theor.) and $3{\cdot}74 \times 10^{-5}$ (exp.), all values in m^2/s.

νR_1^2, νR_1 *and* νR_1^3; *water*. The standard deviation S and the mean error M are respectively (powers of 10 are left out of consideration): $S(\nu R_1^2) = 0{\cdot}95$ and $M(\nu R_1^2) = 0{\cdot}39$, $S(\nu R_1) = 1{\cdot}55$ and $M(\nu R_1) = 0{\cdot}63$, and $S(\nu R_1^3) = 1{\cdot}23$ and $M(\nu R_1^3) = 0{\cdot}50$. It follows that the experimental values of the quantity νR_1^2, which is independent of t_1 in contrast to νR_1 and νR_1^3, approximate more closely to a constant (as predicted by theory) than νR_1 (Jakob [2, 3], empirically for water and carbon tetrachloride) or νR_1^3 (Rallis and Jawurek [4], empirically for water).

It is seen from the five columns at the right-hand side, that the contribution $q_{w,b}$ of the direct vapour formation at the heating surface in water equals the entire increase $q_{w,bi}$ in heat transfer above convection (here a combination of free and forced). This is in contradistinction to the behaviour of the mixtures.

4·1 wt. % *methylethylketone*. Only 10% of the increase is directly due to the bubbles, a result

Table 2. Data are taken at a constant heat flux density $q_w = 44{\cdot}8 \times 10^4$ W/m²

Liquid		Previous estimation [8–11] for released bubbles, but used for bubbles at heating surface						Present theory					
								Bubbles at heating surface			Released bubbles		
	$10^4 C_1$ (m/s$^{\frac{1}{2}}$ degC)	$\Delta T/G_{d,M}$ (degC)	$\Delta T/G_d$ (degC)	$\Delta T = \Delta\vartheta_0$ (degC)	$G_d/G_{d,M}$	$10^3 G_{d,M}$	$10^3 G_d$	ϑ_0 (degC)	$10^2 G_d$	$10^3 G_h^*$	$\Delta\vartheta_0$ (degC)	$10^3 G_d$	$10^4 G_h^*$
Water	24							20	(30·9)	23·6	0·36	(8·8)	6·7
4·1 wt. % methyl-ethylketone	6	375	180	0·6	2·1	1·8	3·7	24	9·3	7·1	0·95	6·1	4·6
1·5 wt. % 1-butanol	18	40	35	0·6	1·2	15	18	21	24·3	18·6	0·14	2·6	2·0
6·0 wt. % 1-butanol	21	35	25	0·6	1·4	17	24	22	29·7	21·5	0·31	6·8	5·2

which is also valid at higher heat flux values approximating the peak flux, (Table 3), since the region of isolated bubbles is extended in this "positive" mixture nearly to peak flux conditions due to the diminished tendency for bubble coalescence (Marangoni effect [12]). This remarkable effect is in quantitative agreement with the present theory, cf. Section 4.3.

The theoretical values of the vaporized fraction at the heating surface are shown in Table 2.

Diffusion. $G_d = (x_0 - x)/(y - x) = (\pi/12)^{\frac{1}{2}}(\rho_2/\rho_1)(C_{1,m}/D^{\frac{1}{2}})\vartheta_0(1 - 1/e)$ denotes the mass fraction according to equation (31), and $G_{d,M} = G_d/[1 + \{(M_1/M_2) - 1\}y_M]$ the corresponding mole fraction.

Table 3. Data are taken at nucleate boiling peak flux conditions

Liquid				Water	4·1 wt. % methyl-ethylketone	1·5 wt. % 1-butanol	6·0 wt. % 1-butanol
Experimental data on vapour bubbles	Wire superheating $\vartheta_{0,\max,e}$		(°C)	21·5	34·0	27·5	
	Wire diameter $10^4 D_w$		(m)	2·00	2·00	2·00	2·00
	Departure radius $10^4 \overline{R}_{1,e}$		(m)	9·2	3·4		
	Wetting constant b_e			0·70	0·90		
	Bubble frequency $\bar{\nu}_e$		(1/s)	70	175		
Maximum density of active nuclei $10^{-4} m_{\max}/A_w$ (1/m²)	Experimental Fig. 1 of Part I			113			
	Geometrical analysis	Equation (57)		199	684		
		Equation (58)		163	442		
	Nucleation Equation (60)			120	710		
	Microlayer Equation (64)			70	395		
Peak flux density $10^{-4} q_{w,\max}$ (W/m²)	Experimental			67	172	169	126
	Theoretical Equation (73)			63	171	157	133
Contributions to peak flux (W/m²) Convection	10^{-4} $q_{w,co,\max}$	Experimental Fig. 1 of Part I		33	51	41·5	40·5
Due to bubbles	10^{-4} $q_{w,bi,\max}$	Theoretical Equation (73)		30	120	115·5	92·5
Direct vapour formation at heating surface $10^{-4} q_{w,b_s\max}$ (W/m²)	Theoretical			30	30		
	Experimental from $\overline{R}_{1,e}$ and $\bar{\nu}_e$			37	26		

Heat. $G_h^* = (C_{1,m}/C_{1,p})(c/1)\vartheta_0(1 - 1/e)$ denotes the mass fraction of the removed equivalent conduction layer at the heating surface according to equation (33).

The ratio $\Delta T/G_d$ determines the growth rate of vapour bubbles in superheated liquid mixtures, cf. equation (12) of Part I of this paper, Section 2.4 and Figs. 2 and 3, and hence the maximal slowing down of bubble growth at a certain low concentration of the more volatile component in binary systems.

The maximum density of active nuclei generating vapour bubbles on a horizontal platinum heating wire at the nucleate boiling peak flux density under atmospheric pressure is shown in Table 3. Note the high population of small bubbles generated at a high average frequency (which has been deduced from Table 1) in the mixture water–methylethylketone. This is associated with a high peak flux $q_{w,\max}$, but also with a low direct vapour formation $q_{w,b,\max} < q_{w,bi,\max} = q_{w,\max} - q_{w,co,\max}$, cf. Section 4.3 and Table 1.

On close inspection, it becomes evident that the considerably increased peak flux in the mixtures is caused directly by the more frequent removal of the thermal boundary layer away from the heating surface, which is successively due to a decreased bubble departure size and a corresponding slowing down of initial bubble growth rates. The subsequent bubble growth after release is only of secondary importance (and can in principle be deduced from the energy balance), in spite of its suitability in studies of the growth of free bubbles on account of the rather uniform superheating of the bulk liquid, cf. Fig. 3.

Résumé—L'ébullition nucléée est décrite comme un phénomène de relaxation concernant la surchauffe de la couche de conduction équivalente à la paroi chauffante due à la croissance rapide des bulles de vapeur successives sur des noyaux d'ébullition actifs. Des expressions pour les temps d'adhérence et de retard, la fréquence des bulles, le rayon de départ, la masse vaporisée et les fractions de diffusion à la paroi chauffante, et le flux maximal d'ébullition nucléée, pourraient ainsi être obtenues. Les prévisions expérimentales séduites des prises de vues à grande vitesse et des courbes d'ébullition des mélanges eau–méthylethylcétone et eau–1-butanol.

De plus, un critère pour le début de l'ébullition par film a été formulé en se basant sur la région d'influence d'une bulle. Les effets du mouillage et de la nucléation sont déterminés et l'on en tient compte dans le traitement théorique. L'avantage des équations actuelles sur les corrélations provenant de l'analyse dimensionnelle est qu'elles mettent en lumière plusieurs phénomènes fortement intéressante qui étaient ignorés auparavant.

Par exemple, la théorie prévoit la coïncidence entre un maximum de la diminution de la vitesse de croissance des bulles et al taille au départ (produisant un minimum de transmission de chaleur aux bulles individuelles: "paradoxe de l'ébullition") et l'existence d'un maximum de flux de point dans l'ébullition nucléée à la même concentration faible du constituant le plus volatil dans un système binaire, qui peut être obtenue à partir des données à l'équilibre. Ceci est aussi en accord avec les résultats expérimentaux.

En principe, les prévisions théoriques contiennent l'effet favorable sur le flux de pointe produit par toutes les méthodes provoquant une diminution de la production de vapeur à la paroi chauffante—ce qui correspond généralement à une augmentation de la fréquence des plus petites bulles—par exemple, l'ébullition de surface, l'écoulement tourbillonnaire, l'emploi de pressions élévées et l'application d'un champ électrostatique.

Zusammenfassung—Das Blassensieden wird als ein Relaxationsphänomen beschrieben, welches für die Überhitzung einer gleichwertigen, leitenden Schicht an der Heizfläche zutrifft, die aufgrund des schnellen Wachstums der von aktiven Keimstellen ausgehenden aufeinanderfolgenden Dampfblasen vorhanden ist.

So konnten Ausdrücke für die Haft- und Verzugszeiten, die Blasenfrequenz, den Ablöseradius, den Dampfmassen- und Diffusionsanteil an der Heizfläche und für die maximale Wärmestromdichte abgeleitet werden. Die theoretischen Vorhersagen sind in guter Übereinstimmung mit Versuchswerten, die von Hochgeschwindigkeitsfilmen und von Siedekurven für Wasser–Methyläthylketon und Wasser–1-Butanol-Gemische hergeleitet wurden.

Zusätzlich wurde ein Kriterium für das beginnende Filmsieden abhängig vom Einflussbereich einer Blase formuliert. Die Einflüsse der Benetzung und der Blasenbildung werden festgestellt und mit in die theoretische Abhandlung aufgenommen.

Der Vorteil der vorliegenden Gleichungen gegenüber Beziehungen, die sich aus der Dimensionsanalyse ergeben, liegt darin, dass sie eine Anzahl hochinteressanter Phänomene aufzeigen, die bisher unbekannt waren.

Zum Beispiel sagt die Theorie eine Übereinstimmung der maximalen Verlangsamung der Blasenwachstumsgeschwindigkeit und der Ablösegrösse (es ergibt sich ein minimaler Wärmeübergang an Einzelblasen: "Siede-Paradoxon") und das Vorhandensein einer maximalen Heizflächenbelastung beim Sieden für die gleiche niedrige Konzentration des flüchtigeren Bestandteils in einem Zweistoff-System vorher, was aus Gleichgewichtsdaten abgeleitet werden kann. Dies stimmt ebenfalls mit Versuchsergebnissen überein. Im Prinzip schliessen die theoretischen Vorhersagen den günstigen Einfluss aller anderen Methoden, die eine verminderte Dampferzeugung an der Heizfläche ergeben, auf die maximale Wärmestromdichte ein, nämlich: Oberflächensieden, Drallströmung, die Verwendung von hohen Drucken und die Anwendung eines elektrostatischen Feldes. Dies entspricht im allgemeinen einer zunehmenden Häufigkeit von kleineren Blasen.

Аннотация—Пузырьковое кипение описывается как явление релаксации, связанное с перегревом эквивалентного проводящего слоя на поверхности нагрева из-за быстрого роста пузырьков пара на активных ядрах.

Таким образом, можно вывести выражение для времени прилипания и запаздывания, частоты пузырьков, отрывного радиуса, количеств испарившейся и диффундировавшей жидкости на поверхности нагрева и критического потока. Теоретические расчеты хорошо согласуются с экспериментальными данными, полученными с помощью киносъёмки и кривых кипения смесей вода–метилэтилкетон и вода–1–бутанол.

Кроме того, сформулирован критерий возникновения пленочного кипения. При проведении теоретического анализа учитывалось влияние смачиваемости и зарождения пузырьков.

Преимущество предлагаемых уравнений перед соотношениями, полученными с помощью анализа размерностей, состоит в учёте ряда весьма интересных явлений, ранее игнорировавшихся.

Теоретические расчёты, например, предсказывают совпадение максимального замедления скорости роста пузырька и отрывного размера (что приводит к минимальной передаче тепла к отдельным пузырькам, т.е. «парадоксу кипения») и появление максимального критического потока при низкой концентрации более летучего компонента бинарной системы. Этот вывод также согласуется с экспериментальными данными.

В принципе теоретические расчёты учитывают благоприятный эффект на критический поток; в результате образование пара на поверхности нагрева снижается, что, в общем, соответствует возрастающей частоте меньших пузырьков.